# Quantum Glass Phases in the Disordered Bose-Hubbard Model

Pinaki Sengupta[1,2] and Stephan Haas[2]

[1]*T-CNLS and NHMFL, Los Alamos National Laboratory, Los Alamos, New Mexico 87545, USA*

[2]*Department of Physics & Astronomy, University of Southern California, Los Angeles, California 90089, USA*

(Received 10 December 2006; published 2 August 2007)

The phase diagram of the Bose-Hubbard model in the presence of off-diagonal disorder is determined using quantum Monte Carlo simulations. A sequence of quantum glass phases intervene at the interface between the Mott insulating and the superfluid phases of the clean system. In addition to the standard Bose glass phase, the coexistence of gapless and gapped regions close to the Mott insulating phase leads to a novel Mott glass regime which is incompressible yet gapless. Numerical evidence for the properties of these phases is given in terms of global (compressibility, superfluid stiffness) and local (compressibility, momentum distribution) observables.

DOI: 10.1103/PhysRevLett.99.050403 PACS numbers: 05.30.Jp, 03.75.Lm, 03.75.Ss, 32.80.Pj

The competition between disorder, interactions, and commensurability in quantum many-body systems is known to produce novel quantum glassy phases, characterized by a gapless spectrum and by the absence of a global order parameter [1]. $^4$He adsorbed on porous media [2], granular superconductors [3], disordered magnets [4] are but a few manifestations of localization effects due to random potentials in interacting bosons. In recent years, ultracold atomic gases in magneto-optical traps have opened a new frontier in the study of strongly correlated systems, as unprecedented control over experimental parameters in these systems makes them ideally suited for studying many-body phenomena. Disorder can be generated in optical lattices by exposure to speckle lasers [5,6], incommensurate lattice-forming lasers [7–9], and by other means [10]. The interplay between disorder and interactions in trapped Bose-Einstein condensates has recently been explored experimentally in $^{87}$Rb, both in the continuum [6,11,12] and in an optical lattice [9,13].

Theoretically, the effects of random potentials on interacting bosons in periodic lattices have been studied using analytic [1,14–16] and numerical techniques [17]. It is now well established that even infinitesimally small potential disorder can destroy the direct superfluid (SF) to Mott insulator (MI) transition in one dimension by introducing an intervening insulating, but compressible, Bose glass (BG) phase [1,18]. Surprisingly, while the effects of potential disorder have been widely investigated, other kinds of disorder, e.g., hopping or interaction strengths, have remained largely unexplored until recently, when it was demonstrated that these can lead to qualitatively quite different phenomena [19–21]. In the quantum rotor model with off-diagonal disorder, the SF to MI transition takes place via an intermediate Mott glass (MG) phase [20,21]—a unique incompressible, yet gapless, glassy regime that was first reported in disordered fermions with extended range interactions [22]. It is thus of great interest to investigate whether such a phase also appears in the Bose-Hubbard model (BHM), and if particle-hole symmetry is essential for the stabilization of such a MG.

We use large-scale quantum Monte Carlo (QMC) simulations to study the effects of off-diagonal disorder in the Bose-Hubbard model on a one-dimensional (1D) lattice. We find that, in contrast to diagonal disorder, the Mott lobes do not shrink in the presence of off-diagonal disorder. Instead, there is an extended BG phase separating the MI lobes from the SF regime, and an additional MG regime emerges.

The Bose-Hubbard model is given by the Hamiltonian

$$H = \sum_{i=1}^{L}\left[ -t_{i,i+1}(b_{i+1}^{\dagger} b_i + \text{H.c.}) + \frac{U}{2} n_i(n_i - 1) - \mu n \right], \tag{1}$$

where $b_i^{\dagger}$ ($b_i$) creates (annihilates) a boson at site $i$, $t_{i,i+1}$ is the hopping matrix element between sites $i$ and $i+1$, $U$ is the on-site interaction strength, and $\mu$ is the chemical potential. Off-diagonal disorder is introduced in the form of a bimodal distribution of the hopping matrix elements—$t_{i,i+1} = t$ or $t/3$ with equal probability [23]. The stochastic series expansion (SSE) [24] method is used to simulate the model (1) in chains of length $L = 64$–$256$. For each set of parameters, 200–1000 realizations of disorder are sampled. To characterize the emerging phases, we compute the superfluid stiffness and the global compressibility. In simulations employing updates that sample different winding number sectors, the stiffness is conveniently obtained from the fluctuations in the winding numbers of the world lines as $\rho_s = [\langle W^2 \rangle / 2\beta]_{\text{av}}$, where $[\ldots]_{\text{av}}$ denotes averaging over multiple realizations of disorder. The global compressibility, $\kappa$, is the energy cost of adding a particle to the system. It is defined by $\kappa = \beta[\langle n^2 \rangle - \langle n \rangle^2]_{\text{av}}$, where $n$ is the density of particles.

At sufficiently large $U$, local variations of the hopping amplitudes create a nontrivial landscape of higher-mobility domains (''lakes'') that coexist with gapped, localized regions. In order to tune the size of these lakes, we introduce spatially correlated disorder. The Fourier filtering method [25] is used to generate a sequence of random numbers, $\eta(i)$, with long-range algebraic correlation,

 

$$C(i-j) \equiv \langle \eta(i)\eta(j)\rangle \sim |i-j|^{-\alpha}. \quad (2)$$

Without any loss of generality, we choose $\alpha = 0.3$. This is then mapped onto a bimodal distribution of hopping integrals, $t_{i,i+1}$, between sites $i$ and $i+1$ of a one-dimensional lattice. While the qualitative features are the same for correlated and random disorder, spatially correlated disorder favors extended domains in the disorder realizations. This, in turn, allows for a more reliable identification of the phase boundaries of the unique MG phase which differs from the MI only in terms of short-range properties. Its proper characterization thus depends crucially on the sampling of finite-ranged domains. With uncorrelated disorder, typical domain sizes are smaller, which renders the MG phase more difficult to detect numerically.

The results of the simulations are summarized in Fig. 1, rendering a rich phase diagram. In the absence of disorder, the ground state of the BHM is in either the SF or the MI phase. The SF-MI transitions (dashed lines) are marked by the simultaneous vanishing of the compressibility, $\kappa$, and stiffness, $\rho_s$, leading to the well-known sequence of MI lobes, with integer fillings [26,27], as $\mu/U$ is varied. In the presence of diagonal disorder, the two transitions—$\rho_s = 0$ and $\kappa = 0$—decouple and a compressible ($\kappa > 0$), insulating ($\rho_s = 0$) BG phase appears. With off-diagonal disorder, an additional glassy phase—the MG—is realized. The MG has global properties identical to the MI ($\rho_s = 0$, $\kappa = 0$ and integer filling), but differs in local properties. In contrast to diagonal disorder, the Mott lobes do not shrink with respect to the clean case. There are no glassy phases in the atomic limit ($t/U \to 0$). At finite $t/U$, the direct SF-MI transitions of the clean limit are replaced by SF-BG-MG-MI sequences. Our results are consistent with all the transitions being continuous.

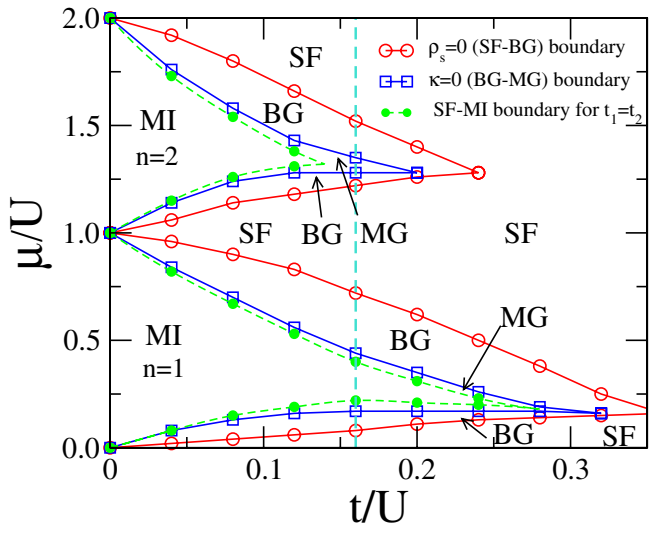


FIG. 1 (color online). Phase diagram of the 1D BHM with spatially correlated off-diagonal disorder: $t_{i,i+1} = t/3$ and $t$ with equal probability. For comparison, the phase boundaries of the clean system ($t_{i,i+1} = t$) are shown with dashed lines. The phases are characterized by the stiffness $\rho_s$ and global compressibility $\kappa$: SF ($\rho_s > 0$, $\kappa > 0$), BG ($\rho_s = 0$, $\kappa > 0$), MI ($\rho_s = 0$, $\kappa = 0$). The MG and MI phases have identical global properties and differ only in local properties.

Details of the simulations are illustrated in Fig. 2. The global stiffness and compressibility are shown as a function of the chemical potential $\mu/U$ at constant $U/t = 6.25$, i.e., along the dashed line in Fig. 1. The data for the clean system are shown for comparison. At small values of $\mu/U$, the ground state is SF with $\rho_s > 0$, $\kappa > 0$. With increasing $\mu/U$, the system passes through a series of phases, as indicated in the figure. The first SF-BG transition is marked by the vanishing of $\rho_s$, while $\kappa$ remains finite across the transition. This coincides with the SF-MI boundary in the clean system with $t_{i,i+1} = t/3$ for all links. In the BG phase, the ground state is a mixture of SF and MI domains of all sizes—the domains with $t_{i,i+1} = t/3$ are local MIs, while those with $t_{i,i+1} = t$ are locally SF. The MI phase of the disordered system coincides with that in the clean limit with $t_{i,i+1} = t$. Of particular interest are the regions marked I, II, and III. For these ranges of $\mu/U$, the global compressibility, $\kappa$, and the stiffness, $\rho_s$, vanish identically. The ground state has integer filling ($n = 1$ for regions I and II and $n = 2$ for region III). The global properties are thus identical to those of the MI phase. As shown next, unlike the MI phase, the ground state has locally compressible regions, and these ranges of $\mu/U$ can accordingly be

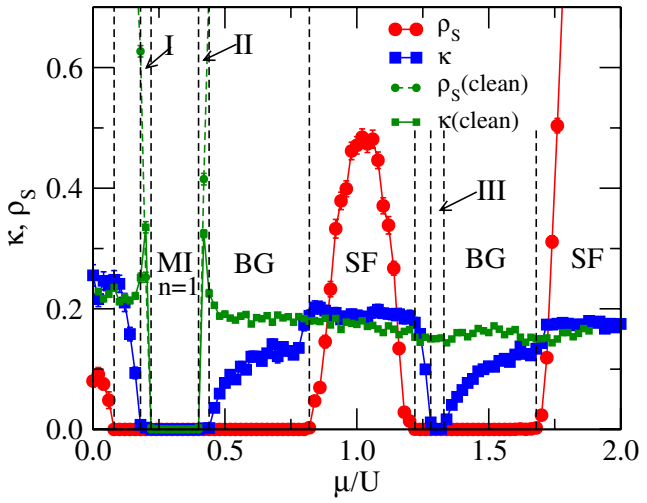


FIG. 2 (color online). Stiffness ($\rho_s$) and compressibility ($\kappa$) as functions of the chemical potential ($\mu$) at constant $t/U = 0.16$ (cut along the dashed line in Fig. 1). For comparison, data of the clean system are also shown. In the absence of disorder, stiffness and compressibility vanish simultaneously at the SF-MI boundary. In the presence of disorder, the $\rho_s = 0$ and the $\kappa = 0$ transitions decouple, resulting in the glassy phases BG ($\rho_s = 0$, $\kappa > 0$) and MG ($\rho_s = 0$, $\kappa = 0$). The MG regimes I, II, and III differ from the MI in terms of local quantities. Note that there is a finite MG phase with $n = 2$ ($1.28 < \mu/U < 1.34$) while there is no corresponding MI phase.

identified as MG phases. Since these regimes lie outside the Mott lobes of the clean system with $t_{i,i+1} = t$ (in particular, there is no $n = 2$ MI phase for this value of $U/t$), the ground state consists of a mixture of SF ($t_{i,i+1} = t$) and MI ($t_{i,i+1} = t/3$) domains as in the BG phase, but differs from the BG by being globally incompressible.

Having explored the global properties, we focus on the local compressibility and the momentum profile of the ground state in each phase. The local compressibility at site $i$ is defined as the local number fluctuation, $\kappa_i = \beta[\langle n_i^2\rangle - \langle n_i\rangle^2]_{\rm av}$, where $n_i$ is the particle density at site $i$. The momentum distribution is obtained from the equal-time Green's function,

$$n(q) = \frac{1}{N}\sum_{l,m} e^{-iq(r_l - r_m)}\langle b_l^\dagger b_m\rangle. \tag{3}$$

$n(q \to 2\pi)$ measures the short-range coherence in the system. The left panel of Fig. 3 shows the distribution of the local compressibilities in a lattice of length $N = 128$, averaged over 800 disorder realizations. In the MI phase, the distribution is peaked at small $\kappa_i$. Conversely, in the SF phase it is peaked at a finite value. In the BG and MG phases, the distribution has a double-peaked structure, consistent with coexisting SF and MI domains in these phases [28]. Figure 3(b), shows momentum profiles in these phases. $n(q)$ is sharply peaked at $q = 0$ in the SF phase and exhibits only a weak broad maximum around $q = 0$ in the MI phase. The behavior of the MG and BG phases is similar and intermediate between the two limits—there is a peak at $q = 0$ arising from the SF domains, but the height is reduced due to the MI domains. Thus the BG and MG phases have very similar short-range structure (both phases consist of coexisting SF and MI domains), although their global responses are rather different, as documented by Fig. 2. While the MG phase is globally incompressible, there exist a gapless channel that allows the exchange of particles between adjacent SF and MI domains, leading to its incompressible yet gapless character. Such a mode is made possible due to the local variation of the kinetic energy of the bosons in the different domains. This explains why the MG phase is not observed for purely diagonal disorder and is unique to off-diagonal disorder [29]. The need to probe local properties also makes it difficult to detect this phase in current optical lattice experiments, where, additionally, domains of different phases coexist. Current developments in local probes using selective microwave spectroscopy [30] and the recently suggested method of using induced controlled interactions between a "probe particle" and the many-body state appear promising [31].

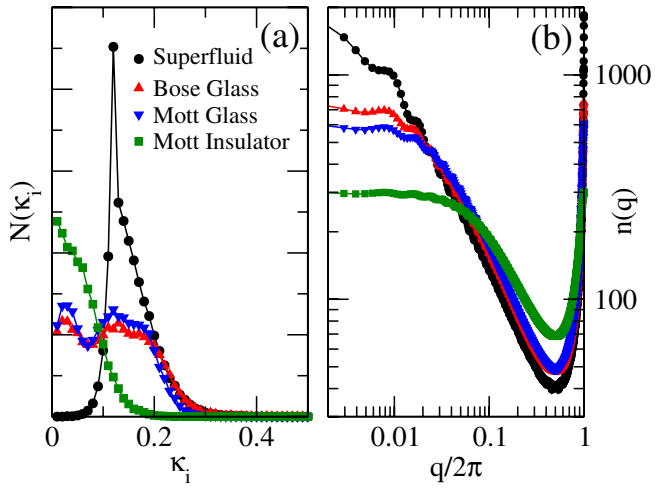


FIG. 3 (color online). (a) The distribution of local (site) compressibilities in the different phases averaged over 800 realizations of disorder. The double-peaked distribution in the BG and MG phases indicate the presence of coexisting SF and MI domains. (b) Momentum profiles of the corresponding ground states. The BG and MG phases have similar momentum profiles, reflecting the similarity in their local structure.

To further characterize the various phases and probe the gapless nature of the MG phase, we study the static structure factor, $S(q)$, for the density-density correlation

$$S(q) = \left[\sum_{j,k} e^{-i\cdot q\cdot(r_j - r_k)}\langle n_j n_k\rangle\right]_{\rm av} \tag{4}$$

and the associated susceptibility,

$$\chi(q) = \left[\int_0^\beta d\tau \sum_{j,k} e^{-i\cdot q\cdot(r_j - r_k)}\langle n_j(\tau) n_k(0)\rangle\right]_{\rm av}. \tag{5}$$

A finite value of $S(q)$ as $q \to 0$ implies the phase is compressible; i.e., the energy gap towards adding or removing a particle vanishes in the thermodynamic limit. Conversely, a vanishing $S(q)$ as $q \to 0$ is a signature of an incompressible phase with a gapped charge excitations. Additionally, the ratio $2\chi(q)/S(q)$ as $q \to 0$ gives an upper bound for the charge excitation gap [32]. Figure 4 shows the structure factor and the susceptibility as a function of momentum for representative points in each of the different phases. Consistent with global compressibility measurements, $S(q)$ vanishes as $q \to 0$ in the MI and MG phases, whereas it remains finite for SF and BG ground states. The upper bound of the charge excitation gap, $\Delta \equiv 2\chi(q)/S(q)$ as $q \to 0$, on the other hand, sheds light on the nature of the MG phase. Although $\Delta_{\rm MG}$ is finite, it is less than the effective chemical potential difference $\delta\mu_{\rm MG}^{I-II}$ between type I ($t = 1$) and type II ($t = 1/3$) domains. While there is a gap towards overall addition or removal of bosons, there exists a gapless mode involving the transfer of particle across the boundaries of the two types of domains which is driven by the effective potential energy difference between adjacent sites at the domain boundaries. This is in contrast to the MI phase where the effective potential difference $\delta\mu_{MI}^{I-II}$ between the two types of domains is less than $\Delta_{\rm MI}$. This confirms the existence of a gapless mode in the MG phase.

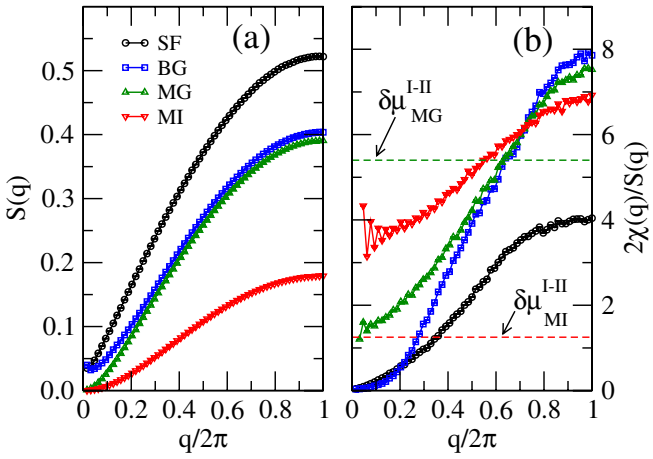


FIG. 4 (color online). (a) Static structure factor, and (b) static susceptibility for the diagonal correlation in the different phases as a function of momentum. The effective potential difference between type I ($t = 1$) and type II ($t = 1/3$) domains in the MG and MI phases are denoted by $\delta\mu_{\mathrm{MG}}^{I-II}$ and $\delta\mu_{\mathrm{MI}}^{I-II}$, respectively. Consistent with global compressibility measurements, $S(q)$ vanishes as $q \to 0$ in the MI and MG phases, but remains finite in the SF and BG phases. $\Delta_{\mathrm{MG}} > 2\chi(q)/S(q)$ as $q \to 0$ in the MG phase, implying the existence of a gapless mode.

In conclusion, using large-scale quantum Monte Carlo simulations, we have observed that off-diagonal disorder (random hopping), yields a nontrivial sequence of quantum glass phases that intervene at the interface between the Mott insulating and the superfluid regimes of the clean system. In particular, the coexistence of gapless and gapped regions close to the Mott insulating phase leads to a novel Mott glass phase which is incompressible and gapless. It shares some of the global properties of the Mott insulator, but resemble the Bose glass in local properties. It is remarkable that the phase boundaries of the Mott insulating phase are basically unaffected by off-diagonal disorder, and that the extent of the Mott glass can be tuned by varying the range of the spatial correlations in the disorder realization. It is also evident that particle-hole symmetry is not a prerequisite for observing the Mott glass phase. The essential ingredients for its realization are off-diagonal (hopping) disorder and commensurate filling. Finally we observe that while the present results are obtained for a one-dimensional system, the Mott glass phase is expected to be more robust in higher dimensions. As seen here, the robustness of the Mott glass phase depends crucially on having large domains with uniform intradomain hopping. This is achieved more readily in higher dimensions due to the increased coordination number. Indeed, in three dimensions, the Mott glass phase is expected to persist to finite temperatures.

We thank T. Roscilde for fruitful discussions. The work was supported by the U. S. DOE under Contracts No. W-7405-ENG-36 (P. S.) and No. DE-FG02-05ER46240 (S. H.). S. H. acknowledges the hospitality of the Los Alamos National Laboratory where part of this work was carried out. The simulations were carried out at the high-performance computing center at USC.

[1] M. P. A. Fisher *et al.*, Phys. Rev. B **40**, 546 (1989).
[2] P. A. Crowell *et al.*, Phys. Rev. Lett. **75**, 1106 (1995).
[3] A. M. Goldman and N. Marković, Phys. Today **51**, No. 11, 39 (1998).
[4] A. Oosawa and H. Tanaka, Phys. Rev. B **65**, 184437 (2002).
[5] P. Horak *et al.*, Phys. Rev. A **58**, 3953 (1998).
[6] D. Clément *et al.*, Phys. Rev. Lett. **95**, 170409 (2005).
[7] B. Damski *et al.*, Phys. Rev. Lett. **91**, 080403 (2003).
[8] A. Sanpera *et al.*, Phys. Rev. Lett. **93**, 040401 (2004).
[9] L. Fallani *et al.*, Phys. Rev. Lett. **98**, 130404 (2007).
[10] R. Folman *et al.*, Adv. At. Mol. Opt. Phys. **48**, 263 (2002).
[11] J. E. Lye *et al.*, Phys. Rev. Lett. **95**, 070401 (2005).
[12] C. Fort *et al.*, Phys. Rev. Lett. **95**, 170410 (2005).
[13] T. Schulte *et al.*, Phys. Rev. Lett. **95**, 170411 (2005).
[14] U. Gavish and Y. Castin, Phys. Rev. Lett. **95**, 020401 (2005).
[15] R. C. Kuhn *et al.*, Phys. Rev. Lett. **95**, 250403 (2005).
[16] A. De Martino *et al.*, Phys. Rev. Lett. **94**, 060402 (2005).
[17] R. T. Scalettar *et al.*, Phys. Rev. Lett. **66**, 3144 (1991).
[18] N. Prokofév and B. Svistunov, Phys. Rev. Lett. **80**, 4355 (1998).
[19] H. Gimperlein *et al.*, Phys. Rev. Lett. **95**, 170401 (2005).
[20] K. G. Balabanyan *et al.*, Phys. Rev. Lett. **95**, 055701 (2005); N. Prokof'ev and B. Svistunov, Phys. Rev. Lett. **92**, 015703 (2004).
[21] E. Altman *et al.*, Phys. Rev. Lett. **93**, 150402 (2004).
[22] E. Orignac *et al.*, Phys. Rev. Lett. **83**, 2378 (1999); T. Giamarchi *et al.*, Phys. Rev. B **64**, 245119 (2001).
[23] In cold atom experiments, implementations of off-diagonal disorder are accompanied by diagonal (potential) disorder. Although we consider only hopping-disorder explicitly, the interaction and on-site (chemical) potential energies are expressed in units of $t$—this results in an implicit realization of diagonal disorder.
[24] A. W. Sandvik, Phys. Rev. B **59**, R14 157 (1999).
[25] H. A. Makse *et al.*, Phys. Rev. E **53**, 5445 (1996).
[26] N. F. Mott, *Metal Insulator Transitions* (Taylor & Francis, London, 1974).
[27] G. G. Batrouni *et al.*, Phys. Rev. Lett. **65**, 1765 (1990).
[28] The finite width of the peaks is due to the finite sizes of the domains, and thus increases with increasing range of the spatial correlations in the disorder.
[29] In a recent work (P. Bounsante *et al.*, arXiv:cond-mat/0611059), the Bose-Hubbard model with uncorrelated off-diagonal disorder was studied using a mean field approach, but no MG phase is reported. A possible reason for this discrepancy may be that one has to explore the local properties to differentiate the MG and MI phases.
[30] G. K. Campbell *et al.*, Science **313**, 649 (2006).
[31] C. Kollath, M. Köhl, and T. Giamarchi, arXiv:0704.1283.
[32] P. C. Hohenberg and W. F. Brinkman, Phys. Rev. B **10**, 128 (1974).